ARTICLE NO. 79-4086

A Tire Runway Interface Friction Prediction Model Concept

Mahinder K. Wahi*
Boeing Commercial Airplane Company, Seattle, Wash.

A thorough literature survey was conducted to establish the range of aircraft tires in use, types of runway surfaces in use, and a list of factors affecting tire-runway interface phenomenon. Both commercial and military aircraft tires and runways were studied. Subsequently, a prediction model has been developed that correlates with existing tire test data to within ±5%. The model consists of a prediction equation expressing the relationships between seven dimensionless groups (pi terms) needed to define the tire-runway interface friction. Due to lack of availability of uniform test data, a tire test program has been recommended to validate the said model.

Introduction

Under a previous effort,[1,2] an airplane braking distance prediction model was formulated using dimensional analysis. The prediction equation had a general format:

$$\left(\frac{Sg}{V^2}\right) = C_\alpha (\mu)^\beta (C_L/C_D)^\gamma (\rho V^6/Feg^2)^\delta$$

where C_α, β, γ, δ are experimental constants, ρ is the air density, and Fe is the engine idle thrust.

The equation permits the calculation of the airplane braking distance S, provided information of airplane and weather parameters and an accurate and meaningful measurement (prediction) of the tire-runway friction coefficient (μ) was available. The use of ground vehicles has been proposed from time to time to assess this crucial element, namely, the aircraft tire to ground available μ. Various efforts have also been made to correlate ground vehicle to aircraft performance without much success.[3] The underlying reason was lack of capability to predict available μ for aircraft as a result of ground μ measurement by vehicles. The correlation required development of a tire model law that related vehicle to aircraft performance. Such a tire model concept has now been developed and results are reported in Ref. 4. This paper is based on relevant information extracted from the Ref. 4 report. It should be noted that the concept is only a first step and needs to be verified further by proper tire test data.

Figures 1 and 2 show the basic concept used to arrive at the tire model. A literature survey establishes the range of tire parameters, runway parameters, and variables affecting the interface friction. A dimensional analysis technique is then used to obtain dimensionless groups or π terms. Statistical curve-fitting techniques are used to obtain intra-pi-term relationships or component equations which are combined to yield the final prediction equation(s). Available tire test data (obtained through a literature survey) is then correlated with this prediction model.

Literature Survey

The tire survey encompassed the following:

1) Type VII or equivalent (new design, Type VIII, etc.) tires.
2) Airplanes with skid control systems only.
3) Main gear tire characteristics only.
4) Rated values for load, inflation pressure and speed considered. The opeational values are different (data not readily available).
5) All major airplanes in military and commercial use.

The information was compiled from Refs. 5-10 and is summarized in Table 1. Detailed tables of this survey may be found in Ref. 4.

The runway/airport survey applies as follows:

1) Top 100 U.S. commercial airports only.
2) All United States Air Force active bases.
3) All naval facilities included.
4) All army air facilities included.
5) Only the longest runway for each airport considered.
6) Texture depth measured by grease/sand patch method.

The information was compiled from Refs. 11-17 and is summarized in Table 2. Detailed tables of this survey are included in Ref. 4.

An appreciation of the factors that may influence road hold may be gained from Table 3. This model representing tire road hold has been derived by Holmes, et al,[18] from the variables listed by a number of authors as being important in the road hold phenomenon. There are four main factors influencing road hold: tire, pavement, lubricant, and operating condition. These have been subdivided into forty-eight variables. Some of these variables within each of the groups interrelate with others in the group and even with variables outside the group. Many of the individual variables illustrated could be further subdivided.[19,20]

Due to the apparent complexity of the problem, it was decided to limit the scope of the present analysis by considering only: wet runways (only water, no rubber, dirt, salt, oil deposits, etc.); braked rolling (no yawed rolling/directional control); peak μ or μ-max. (no locked wheel situations); and texture depth (no individual asperities, shape, roundness, arrangement, etc.).

Table 1 Range of type VII aircraft tire parameters[a]

Parameter	Range	Airplane
Tire size, in.	18×5.5-56×16	Lear jet-B-52
Aspect ratio	0.66-0.91	F4-F-14
Speed, mph	175-275	A7A-F104
Inflation pressure, psi	100-360	Lear jet-F4B
Loads, lb	4000-76,000	Lear jet-B-52

[a]Common parameters: cross-ply design, reinforced rib (RR), 4 or 5 circumferential grooves, tubeless, natural rubber base, and used on main gears.

Received Aug. 3, 1978; revision received Nov. 16, 1978.

Index categories: Analytical and Numerical Methods; Deceleration Systems; Landing Dynamics.

*Senior Engineer, Landing Gear Systems.

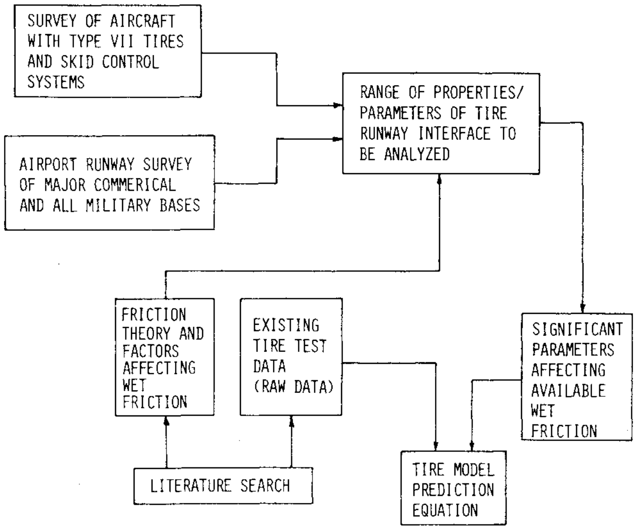

Fig. 1 Tire correlation concept.

This helped reduce the number of variables to be considered for model formulation. The list of parameters was further trimmed down by grouping interrelated variables and excluding those having more relevance to fluid drag and spray patterns rather than friction force. Some parameters, although important, could not be included in the final model because no relevant test data existed, e.g., viscosity and density variation of contaminant mixtures.

Selection of Pertinent Parameters

Figure 2 is a flow chart where each block represents a major step of analysis in the formulation of the prediction equation.

Table 4 lists significant parameters after excluding those that are outside the scope of the present work and for reasons spelled out earlier. The following paragraphs present reasons for further refinement to the list.

A. Tire Tread Compound

Pneumatic tires usually contain a variety of rubber compositions, each designed to contribute some particular factor of overall performance. Rubber compounds designed for a specific function will usually be similar but not identical in composition and properties, although in some cases there can be significant differences between compounds in tires of various types. The guiding principle in development of rubber compositions for tires is to achieve the best balance of properties for a particular type of tire service.[21]

Tire manufacturers over the years have each developed their own tread compounding mixes and formulas and consider this as proprietary information. However, it is recognized that all aircraft tires are manufactured from natural rubber-based polymers and their compounding from one manufacturer to the next does not vary extensively. Therefore, it is not considered as an independent variable for model formulation.

Table 2 Range of runway parameters

Surface	asphalt	or	concrete
Treatment[a]	plant mix conventional grooved slurry seal		Marshal asphalt German antiskid coat porous friction course crushed rock
Texture depth	0.004 in. (0.10 mm)	to	0.09 in. (2.25 mm)

[a] Treatment applicable to asphalt and/or concrete.

B. Fluid Viscosity and Density

As stated under various versions of the 3-zone concept (Refs. 18, 22, 23 and Fig. 3), the retarding forces developed in zones 1 and 2 are dependent respectively upon the density and viscosity of the fluid. However, their contribution to the friction is much smaller than that of zone 3 where the bulk of effective retarding force is generated. The variation of these two parameters should be that of the viscosity and density of the contaminated mixture of rain water, sleet, grit, mud, salt, detritus, grease, tire rubber, fuel, and so on. No meaningful test data are available even for individual contaminants. As a result, they cannot presently be considered as independent variables for the model. However, during dimensional analysis, density is retained for dimensional homogeneity and not as an independent variable.

C. Pavement Texture

A number of researchers have generally agreed that large-scale (macro) texture largely affects the rate at which friction decreases with increased speed.[24] On the other hand, the level of friction at a given speed, particularly at low speeds, was mainly a function of the fine-scale (micro) texture. Microtexture has been generally considered an inherent characteristic of individual aggregate particles, whereas

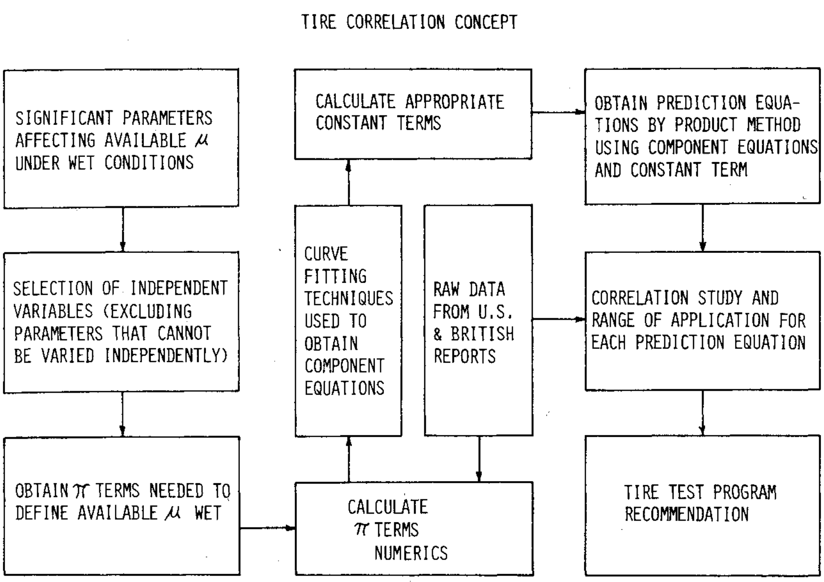

Fig. 2 Block diagram for analysis.

Table 3 Interrelating factors that contribute to the road hold phenomenon

Tire	Pavement
1. Tire load	25. Type
2. Tire inflation pressure	26. Surface texture
3. Tire size	27. Microtexture
4. Tire construction and design	28. Macrotexture
5. Tire tread pattern design	29. Resistance to polishing by traffic
6. Chemical formulation	30. Resistance to abrasion and crushing strength
7. Polymer type	31. Weathering characteristics
8. Carbon black type	32. Temperature
9. Curing system	33. Thermal properties
10. Other ingredients of tread compound	34. Matrix properties
11. Physical properties	35. Contamination
12. Tread surface conditions	36. Grooving
13. Surface degradation	
14. Chemical/physical absorption	Operating conditions
15. Thermal properties	37. Traffic density
16. Dynamic properties	38. Velocity
17. Surface temperature	39. Tire slip, peak, or locked-wheel conditions
	40. Site design
Lubricant	41. Prevailing climatic conditions
18. Type	42. Testing vehicle design
19. Viscosity	43. Method of measurement
20. Surface tension	44. Stopping distance
21. Film depth	45. Decelerometer
22. Film strength	46. Cornering force coefficient
23. Temperature	47. Braking force coefficient
24. Impurities	48. Towed vehicle (impending slide)

Table 4 Significant parameters

Tire
1. Tire load
2. Tire inflation pressure
3. Tire size
4. Tire construction and design
5. Tire tread pattern
6. Tire tread compound
7. Polymer type (natural, synthetic)
8. Surface degradation (tread wear)
Lubricant
9. Viscosity
10. Density
11. Film depth
Pavement
12. Microtexture
13. Macrotexture
14. Resistance to polishing by traffic
15. Resistance to abrasion and crushing strength
16. Weathering characteristics
17. Temperature
Operating Conditions
18. Velocity
19. Tire slip, peak, or locked-wheel conditions
20. Braking force coefficient

Table 5 Pertinent parameters

Variables	Notation
Peak available mu	μ
Forward ground speed	V
Tire inflation pressure	p
Tire tread depth	d_{tr}
Tire outside diameter	D
Tire width	w
Tire vertical load	Z
Runway macrotexture depth	d_{tx}
Fluid depth	h
Fluid density	ρ[a]

[a] Included only for dimensional homogeneity, not as an independent variable.

macrotexture was taken as the roughness of the aggregate matrix combination.

Surface texture effects on μ are treated in the literature[20,25] by presenting curves for typical surfaces, e.g., A for smooth, B for lightly textured, C for heavily textured, D for shallow grooved, and E for deep-grooved concrete and asphalt surfaces (see Figs. 4 and 5).

These represent classes of runway with different surface macrotexture depths but all with essentially harsh microtextures. Figure 5 lists macrotexture depths for a large number of runways and divides these into five classes; the average texture depth of each class is approximately that represented by the corresponding typical surface. The data sources for compiling Fig. 5 are Refs. 11 and 26-31.

An illustration of the effect of a smooth microtexture is given in Fig. 6. Such situations can arise if 1) A runway is constructed using a rounded or polished gravel aggregrate—a comparatively rare event. 2) A roadway is used as a runway, since the higher traffic density on roads makes polishing of the surface material a severe problem. 3) A runway has large areas of smooth polished surface. In light of the preceding discussion, it was decided to use the runway macrotexture depth as the independent surface parameter.

D. Other Parameters

Loss of friction is usually most severe during the first two years after construction.[32] Thereafter, the rate of polishing decreases and eventually reaches a stable level of smoothness. Most runways in use today are at least two years old. Thus, factor 29 in Table 3 can be eliminated as an independent variable.

The only form of rubber abrasion under wet conditions, called scoring,[18] is related to the content of carbon black in the tread. In the absence of any meaningful quantitative data, its inclusion is not justified. Finally, weathering and pavement temperature effects on friction have been shown to be related to the surface texture, already included in the list.

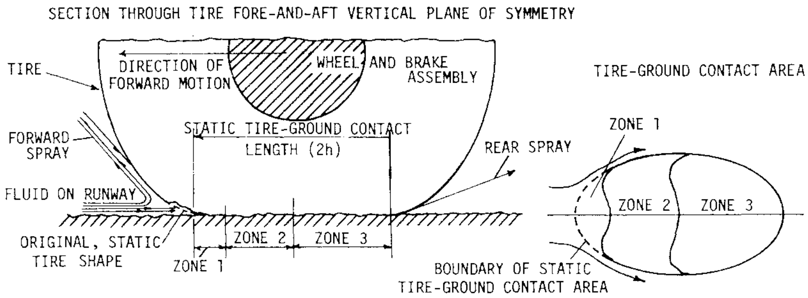

Fig. 3 Three-zone concept.

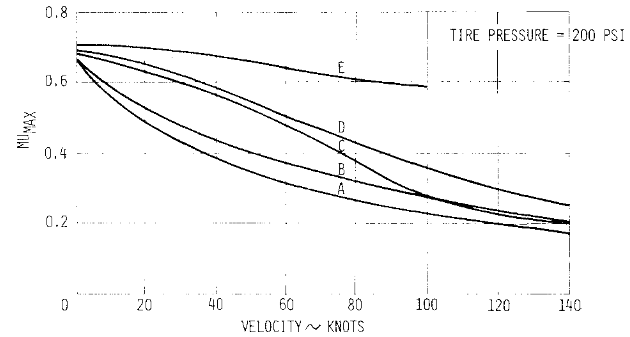

Fig. 4 mu_{max} —velocity curves for various surfaces.

The parameters not discussed in the preceding paragraphs are independent variables and are included in the final list of the pertinent variables (Table 5).

Development of Prediction Model

A. Dimensional Equation

Having identified the pertinent and independent variables (Table 5), the first and most important step in forming a prediction model has been completed. The second step is to express the dependent variable as a function of the independent variables so that:

$$\mu = F(V, p, d_{tr}, D, w, Z, d_{tx}, h, \rho) \tag{1}$$

The dimensional matrix that can be formed for the fundamental units (mass, length, and time) of the ten parameters in Eq. (1) is of rank 3, so that, according to Buckingham's π theorem,[33] these would yield seven independent π terms. By inspection and analysis, they can be written:

$$\pi_1 = (\mu),\ \pi_2 = (d_{tx}/D),\ \pi_3 = (d_{tr}/D),\ \pi_4 = (h/D),$$

$$\pi_5 = (D-d)/2w,\ \pi_6 = (Z/pD\sqrt{wD}),\ \text{and}\ \pi_7 = (\rho V^2 D^2/Z)$$

where d is the wheel diameter and $(D-d)/2w$ is defined as the tire aspect ratio.

Thus,

$$(\mu) = F\left\{\frac{d_{tx}}{D}, \frac{d_{tr}}{D}, \frac{h}{D}, \frac{D-d}{2w}, \frac{Z}{pD\sqrt{wD}}, \frac{\rho V^2 D^2}{Z}\right\} \tag{2a}$$

or

$$(\pi_1) = F(\pi_2, \pi_3, \pi_4, \pi_5, \pi_6, \pi_7) \tag{2b}$$

The application of dimensional analysis, including the π theorem, leads to a type of equation involving an unknown function, of which Eq. (2a) is an example. Before a prediction equation can be formulated, the nature of the function must be determined.

The general nature of the function can be shown to be[33]:

$$a = C_\alpha a_1^{C_1} a_2^{C_2} a_3^{C_3} \text{-------} a_n^{C_n} \tag{3}$$

in which the dependent variable a is expressed as a dimensionless coefficient (C_α) multiplied by the product of the pertinent independent variables, each raised to the appropriate power. The nature of coefficient C_α must be determined experimentally. Also, the exponents, C_1, C_2, etc., are to be determined from test data.

B. Literature Search for Existing Tire Test Data

The complexity of friction phenomenon is evident from the number of variables involved. To date it has not been possible to express many of these quantities in rigorous form. It is, therefore, the practice of authors to simply describe all materials and geometry of test devices together with test results.[34] The nature of present study necessitated the sorting

Table 6 Runway texture depth vs μ data (π_2 vs π_1)

Texture depth, d_{tx}-in.	$d_{tx}/D \times 10^3$ or (π_2)	μ or (π_1) @ velocity in knots				Runway surface[a]	Basic data
		25	50	75	100		
0.0012	0.037	0.165	0.082	0.059	0.047	SC	$D = 32$ in.
0.0013	0.041	0.153	0.100	0.071	0.059	SC	$h = 0.1$-0.2 in.
0.0017	0.053	0.110	0.080	0.060	0.050	SC	$p = 140$ psi
0.0059	0.184	0.382	0.235	0.129	0.059	TC	$z = 12{,}000$ lb
0.0067	0.209	0.459	0.300	0.165	0.071	TC	A. R. = 0.842
0.0078	0.244	0.550	0.395	0.225	0.090	TC	All rubber, (National Rubber) tread and new
0.0096	0.300	0.647	0.412	0.259	0.071	SAA	
0.0135	0.422	0.795	0.600	0.370	0.100	SAA	
0.0220	0.687	0.830	0.685	0.475	0.190	LAA	

[a] SC = smooth concrete, TC = textured concrete, SAA = small aggregate asphalt, and LAA = large aggregate asphalt [data source: Ref. (28)]

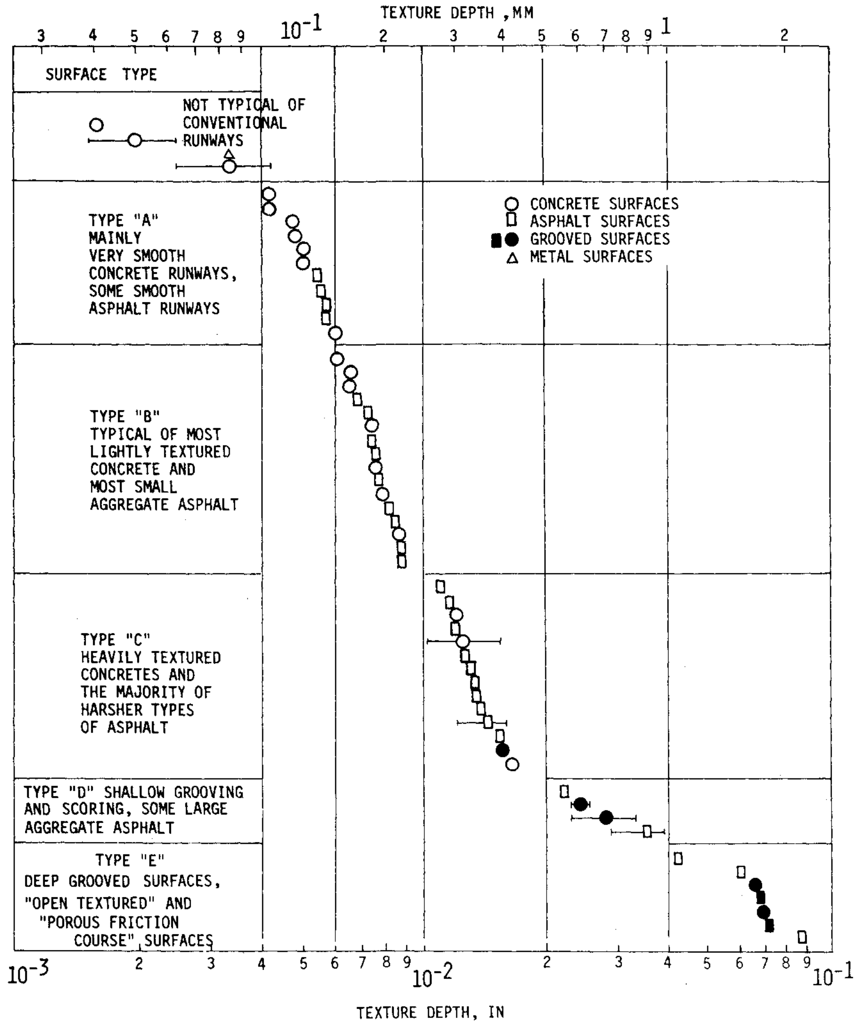

Fig. 5 Classification of runway surfaces: texture depths measured by grease or sand patch methods (adapted from Ref. 25).

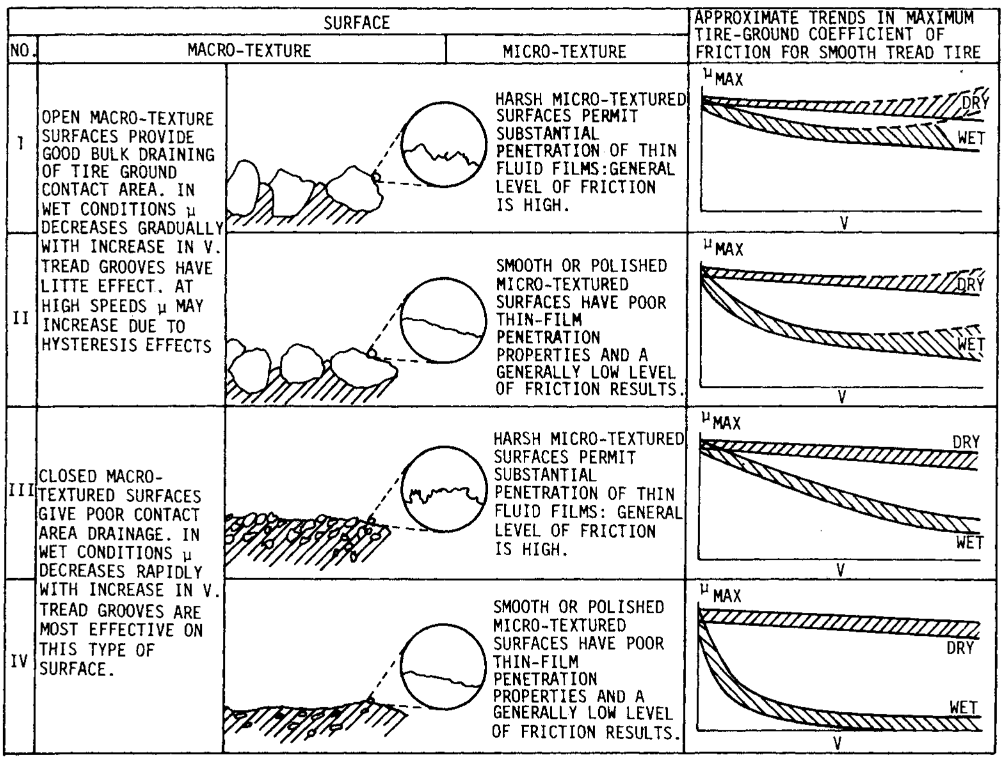

Fig. 6 Effect of surface texture on tire-ground coefficient of friction (adapted from Ref. 25).

of the wide range of conditions that influence available friction and then make an attempt to express the magnitude of each effect. Unfortunately, the influence of runway surface variables is usually measured by one type of test, tire variables by another type of test, and other variables by a third.

With this in mind, a thorough literature survey in the general area of tire-road interaction was undertaken with an intention to extract as much usable data (for model use) as possible. An example of the resulting tire test data extracted from Ref. 28 is shown in Table 6. Similarly, data for other π terms were extracted as follows:

Relationship between	Extracted from Ref.
π_1 vs π_3	35
π_1 vs π_4	36
π_1 vs π_5	37,38
π_1 vs π_6	25
π_1 vs π_7	25

Numerous other test data are available but cannot be used for the model under consideration. Even though attempts were made to use only aircraft tire test data, some automotive tire data had to be included, e.g., π_1 vs π_4 as no such data are available for aircraft tires. Also, the automotive tire data used are for μ-skid (locked-wheel) conditions, while all other data are μ-peak type. Virtually no aircraft test data and very little on automotive tires[39] are available on the aspect ratio effects. Data for model use were therefore, generated from two test points available at each speed which show a trend similar to that shown in the Ref. 39 study.

Many other prudent engineering judgments had to be made as to the quantitative nature of basic test data required for model verification but missing from the test reports containing the subject data. Caution must, therefore be practiced, such that the material presented in this report is used only in its technical context, i.e., as a working concept, and not in its numerical content until further model verification has been conducted, e.g., through recommendations for controlled conditions tire-testing.

C. Component Equations

The best procedure for evaluating a function is to arrange the observations so that all but one of the π terms containing the independent variables in the function remain constant. Then the remaining independent π term is varied to establish a relationship between it and the dependent variable (π_1) term. This procedure is repeated for each of the π terms in the function; the resulting relationships between π_1 and the other individual π terms are called component equations. Statistical curve-fitting computer programs were used to generate the

Table 7 Summary of component equations

V-knots	Equation	Eq. no.	Type of surface[c]
25[a]	$(\pi_1)=1.3757(\pi_2)^{0.7046}$	(7-1)	A, C, E
25	$(\pi_1)=0.4659(\pi_3)^{0.1200}$	(7-2)	A, C, E
25	$(\pi_1)=0.3650(\pi_4)^{-0.0714}$	(7-3)	A
25	$(\pi_1)=0.4246(\pi_4)^{-0.0742}$	(7-4)	C
25	$(\pi_1)=0.3990(\pi_4)^{-0.1518}$	(7-5)	E
25	$(\pi_1)=0.4098(\pi_5)^{0.3089}$	(7-6)	A, C, E
25	$(\pi_1)=0.5536(\pi_6)^{0.1117}$	(7-7)	A
25	$(\pi_1)=0.7633(\pi_6)^{0.1665}$	(7-8)	C
25	$(\pi_1)=0.8890(\pi_6)^{0.1855}$	(7-9)	E
50 psi[b]	$(\pi_1)=0.3473(\pi_7)^{-0.3129}$	(7-10)	A
50	$(\pi_1)=0.4466(\pi_7)^{-0.2443}$	(7-11)	C
50	$(\pi_1)=0.7150(\pi_7)^{-0.06403}$	(7-12)	E

[a]Similar equations were formulated for $V=50$, 75 and 100 knots. [b]Similar equations were formulated for $p=100$, 200, and 300 psi. [c]A = very smooth concrete/asphalt surfaces, C = heavily textured surfaces, and E = deep-grooved surfaces.

Table 8 Reduced list of prediction equations

Surface type	V_{π_7}	Average of four prediction equations
A	25	$(\pi_1)=1.1619(\pi_2)^{.7046}(\pi_3)^{.1200}(\pi_4)^{-.0714}(\pi_5)^{.3089}(\pi_6)^{.1117}(\pi_7)^{-.2609}$
C		$(\pi_1)=1.3039(\pi_2)^{.7046}(\pi_3)^{.1200}(\pi_4)^{-.0742}(\pi_5)^{.3089}(\pi_6)^{.1665}(\pi_7)^{-.2410}$
E		$(\pi_1)=1.4157(\pi_2)^{.7046}(\pi_3)^{.1200}(\pi_4)^{-.1518}(\pi_5)^{.3089}(\pi_6)^{.1855}(\pi_7)^{-.0494}$
A	50	$(\pi_1)=0.9470(\pi_2)^{.7887}(\pi_3)^{.2501}(\pi_4)^{-.3347}(\pi_5)^{.6450}(\pi_6)^{.2002}(\pi_7)^{-.2609}$
C		$(\pi_1)=1.1566(\pi_2)^{.7887}(\pi_3)^{.2501}(\pi_4)^{-.1864}(\pi_5)^{.6450}(\pi_6)^{.1602}(\pi_7)^{-.2410}$
E		$(\pi_1)=1.0724(\pi_2)^{.7887}(\pi_3)^{.2501}(\pi_4)^{-.1773}(\pi_5)^{.6450}(\pi_6)^{.1482}(\pi_7)^{-.0494}$
A	75	$(\pi_1)=0.6731(\pi_2)^{.7265}(\pi_3)^{.2234}(\pi_4)^{-.4113}(\pi_5)^{1.3555}(\pi_6)^{.2204}(\pi_7)^{-.2609}$
C		$(\pi_1)=0.5840(\pi_2)^{.7265}(\pi_3)^{.2234}(\pi_4)^{-.3820}(\pi_5)^{1.3555}(\pi_6)^{.1257}(\pi_7)^{-.2410}$
E		$(\pi_1)=0.4494(\pi_2)^{.7265}(\pi_3)^{.2234}(\pi_4)^{-.4004}(\pi_5)^{1.3555}(\pi_6)^{.1254}(\pi_7)^{-.0494}$
A	100	$(\pi_1)=0.1789(\pi_2)^{.3361}(\pi_3)^{.1192}(\pi_4)^{-.5376}(\pi_5)^{3.0071}(\pi_6)^{.1942}(\pi_7)^{-.2609}$
C		$(\pi_1)=0.1657(\pi_2)^{.3361}(\pi_3)^{.1192}(\pi_4)^{.4645}(\pi_5)^{3.0071}(\pi_6)^{.0992}(\pi_7)^{-.2410}$
E		$(\pi_1)=0.1302(\pi_2)^{.3361}(\pi_3)^{.1192}(\pi_4)^{-.4254}(\pi_5)^{3.0071}(\pi_6)^{.1110}(\pi_7)^{-.0494}$

component equations. A summary of the equations is listed in Table 7.

D. Generalized Functions

When the component equations have been determined, they are combined in a certain manner to give a general relationship. It is possible for some of the component equations to be combined by multiplication, while others require addition in the formation of the resultant prediction equation. For the problem on hand, the nature of available data (multiple sources, variety of test conditions, both automotive and aircraft tires, laboratory and actual runway tests, etc.) prevented a rigorous analysis as to which of the two methods should be used. Based on past experience,[1,2] it was decided to use the multiplication method. The necessary and sufficient conditions to be met for the function to be a product were developed and translated into tests of validity. Again, these tests of validity cannot be tried until a systematic set of data under controlled test conditions (i.e., data obtained for all π terms on one tire, one surface, etc.) is made available.

It can be shown that when the component equations (see Table 7) are combined by multiplication, the prediction equation is of the form[4]:

$$(\pi_1) = \{(C)(\pi_1)_{\bar{3}-\bar{7}}(\pi_1)_{\bar{2},\bar{4}-\bar{7}}(\pi_1)_{\bar{2},\bar{3},\bar{5}-\bar{7}} \times (\pi_1)_{\bar{2}-\bar{4},\bar{6},\bar{7}}(\pi_1)_{\bar{2}-\bar{5},\bar{7}}(\pi_1)_{\bar{2}-\bar{6}}\} \tag{4}$$

where the overbar denotes a constant (held) value, and $3 \rightarrow 7$ means 3,4,5,6,7.

The analysis shows that the value of the constant term C is of the form:

$$C = \frac{1}{[F(\bar{\pi}_2 \rightarrow \bar{\pi}_7)]^5} \tag{5}$$

Thus, the prediction equation is of the form:

If the supplementary sets of data satisfy either Eq. (7a) or (7b), the general equation can be formed by multiplying the component equations together and dividing by the constant, as indicated in Eq. (6).

Another test of validity is to calculate the value of the constant C of Eq. (4). The test requires that any of the six component equations in a set [e.g., (7-1, 7-2, 7-3, 7-6, 7-7, and 7-10)] should yield an identical value for C. The value of constant C for each prediction equation was calculated from a product function of the values generated by six component equations of each set. It should be emphasized here that these values of constants are theoretical and that the true values can only be generated from a complete set of controlled test conditions. The calculated values of C for the three possible prediction equations combinations are:

Equations combined	C
7-1, -2, -3, -6, -7, -10	59.77
1 2 4 6 8 11	34.18
1 2 5 6 9 12	20.94

The prediction equations were thus formed and are shown in Table 8. Each of these twelve equations is applicable to a type of surface, i.e., A, C, or E and a given velocity, i.e., 25, 50, 75, or 100 knots. The next logical step was to determine if these equations were interchangeable for a given type of surface, i.e., each equation being applicable for the full velocity range. The analysis showed that this could be achieved with full success in some equations and with partial success in others by modifying the velocity π term. Accordingly, applicable equations were modified and are shown in Table 9.

Model to Raw-Data Correlation

The prediction equations were next used to correlate back with raw data used in the model formulation. A summary of errors in correlation is listed in Table 10.

$$F(\pi_2 \rightarrow \pi_7) = [F(\pi_2,\bar{\pi}_3 \rightarrow \bar{\pi}_7)F(\pi_3,\bar{\pi}_2 \rightarrow \bar{\pi}_7)F(\pi_4,\bar{\pi}_2 \rightarrow \bar{\pi}_7)F(\pi_5,\bar{\pi}_2 \rightarrow \bar{\pi}_7)F(\pi_6,\bar{\pi}_2 \rightarrow \bar{\pi}_7)F(\pi_7,\bar{\pi}_2 \rightarrow \bar{\pi}_6)]/[F(\bar{\pi}_2 \rightarrow \bar{\pi}_7)]^5 \tag{6}$$

The equations constituting a test for the validity of Eq. (6) are shown to be[4]

$$[F(\pi_2,\bar{\pi}_3 \rightarrow \bar{\pi}_7)F(\pi_3,\bar{\pi}_2 \rightarrow \bar{\pi}_7)F(\pi_4,\bar{\pi}_2 \rightarrow \bar{\pi}_7)F(\pi_5,\bar{\pi}_2 \rightarrow \bar{\pi}_7)F(\pi_6,\bar{\pi}_2 \rightarrow \bar{\pi}_7)]/[F(\bar{\pi}_2 \rightarrow \bar{\pi}_7)]^5$$
$$\equiv [F(\pi_2,\bar{\pi}_3 \rightarrow \bar{\bar{\pi}}_7)F(\pi_3,\bar{\pi}_2 \rightarrow \bar{\bar{\pi}}_7)F(\pi_4,\bar{\pi}_2 \rightarrow \bar{\bar{\pi}}_7)F(\pi_5,\bar{\pi}_2 \rightarrow \bar{\bar{\pi}}_7)F(\pi_6,\bar{\pi}_2 \rightarrow \bar{\bar{\pi}}_7)]/[F(\bar{\pi}_2 \rightarrow \bar{\bar{\pi}}_7)]^5 \tag{7a}$$

or

$$[F(\pi_3,\bar{\pi}_2 \rightarrow \bar{\pi}_7)F(\pi_4,\bar{\pi}_2 \rightarrow \bar{\pi}_7)F(\pi_5,\bar{\pi}_2 \rightarrow \bar{\pi}_7)F(\pi_6,\bar{\pi}_2 \rightarrow \bar{\pi}_7)F(\pi_7,\bar{\pi}_2 \rightarrow \bar{\pi}_6)]/[F(\bar{\pi}_2 \rightarrow \bar{\pi}_7)]^5$$
$$\equiv [F(\pi_3,\bar{\bar{\pi}}_2 \rightarrow \bar{\pi}_7)F(\pi_4,\bar{\bar{\pi}}_2 \rightarrow \bar{\pi}_7)F(\pi_5,\bar{\bar{\pi}}_2 \rightarrow \bar{\pi}_7)F(\pi_6,\bar{\bar{\pi}}_2 \rightarrow \bar{\pi}_7)F(\pi_7,\bar{\bar{\pi}}_2 \rightarrow \bar{\pi}_6)]/[F(\bar{\bar{\pi}}_2 \rightarrow \bar{\pi}_7)]^5 \tag{7b}$$

The values $\bar{\bar{\pi}}_2$ and $\bar{\bar{\pi}}_7$ are values of π_2 and π_7 held constant at some value other than $\bar{\pi}_2$ and $\bar{\pi}_7$. Thus, from the observed data:

$$\bar{\pi}_7 = \frac{\rho V^2 D^2}{Z} \text{ @ } V = 25 \text{ knots} \quad \text{the primary set of data for example}$$

$$\bar{\pi}_7 = \frac{\rho V^2 D^2}{Z} \text{ @ } V = 25 \text{ knots} \quad \text{the primary set of data for example}$$

$$\left.\begin{aligned} \bar{\bar{\pi}}_7 &= \frac{\rho V^2 D^2}{Z} \text{ @ } V = 50 \text{ knots} \\ \bar{\bar{\bar{\pi}}}_7 &= \frac{\rho V^2 D^2}{Z} \text{ @ } V = 75 \text{ knots} \\ \bar{\bar{\bar{\bar{\pi}}}}_7 &= \frac{\rho V^2 D^2}{Z} \text{ @ } V = 100 \text{ knots} \end{aligned}\right\} \text{supplementary sets of data}$$

For a given surface (type), the three prediction equations are interchangeable, alternate solutions. Thus Eqs. (9-1, 9-4, and 9-7) are interchangeable, although their prediction accuracies are different at different velocities (see Table 10). Similarly Eqs. (9-2, 9-5, and 9-8) are interchangeable and so are Eqs. (9-3, 9-6 and 9-9). Equations (9-4, 9-5, and 9-6) yield the best results for the three surfaces at all velocities and are, therefore, the best solutions for use.

The formulation of the prediction equation has been accomplished with the use of dimensional analysis. A complex dynamic process has been defined by means of dimensional terms and the resulting equation appears with the general format

$$(\mu) = C_\alpha (d_{tx}/D)^\beta (d_{tr}/D)^\gamma (h/D)^\delta \times [(D\text{-}d)/2w]^\epsilon (Z/pD\sqrt{WD})^\zeta (\rho V^2 D^2/Z)^\eta$$

Table 9 Summary of prediction equations

Surface type	V^{*a} knots	Equation	Equation number
A	25	$(\pi_1)=1.1619(\pi_2)^{.7046}(\pi_3)^{.1200}(\pi_4)^{-.0714}(\pi_5)^{.3089}(\pi_6)^{.1117}(\pi_7)^{-(.2609+.00946\Delta V)}$	9-1
C	25	$(\pi_1)=1.3039(\pi_2)^{.7046}(\pi_3)^{.1200}(\pi_4)^{-.0742}(\pi_5)^{.3089}(\pi_6)^{.1665}(\pi_7)^{-(.2410-.00076\Delta V+.00023\Delta V^2)}$	9-2
E	25	$(\pi_1)=1.4157(\pi_2)^{.7046}(\pi_3)^{.1200}(\pi_4)^{-.1518}(\pi_5)^{.3089}(\pi_6)^{.1855}(\pi_7)^{-(.0493+.00916\Delta V+.00024\Delta V^2)}$	9-3
A	50	$(\pi_1)=\ .9470(\pi_2)^{.7887}(\pi_3)^{.2501}(\pi_4)^{-.3347}(\pi_5)^{.6450}(\pi_6)^{.2002}(\pi_7)^{-(.2619+.00988\Delta V)}$	9-4
C	50	$(\pi_1)=1.1566(\pi_2)^{.7887}(\pi_3)^{.2501}(\pi_4)^{-.1864}(\pi_5)^{.6450}(\pi_6)^{.1602}(\pi_7)^{-(.2345+.0007\Delta V+.0004\Delta V^2)}$	9-5
E	50	$(\pi_1)=1.0724(\pi_2)^{.7887}(\pi_3)^{.2501}(\pi_4)^{-.1773}(\pi_5)^{.6450}(\pi_6)^{.1482}(\pi_7)^{-(.0468+.01184\Delta V+.0004\Delta V^2)}$	9-6
A	75	$(\pi_1)=\ .6731(\pi_2)^{.7265}(\pi_3)^{.2234}(\pi_4)^{-.4113}(\pi_5)^{1.3555}(\pi_6)^{.2204}(\pi_7)^{-(.2612+.0194\Delta V-.000193\Delta V^2)}$	9-7
C	75	$(\pi_1)=\ .5840(\pi_2)^{.7265}(\pi_3)^{.2234}(\pi_4)^{-.3820}(\pi_5)^{1.3555}(\pi_6)^{.1257}(\pi_7)^{-(.2411+.05315\Delta V-.000834\Delta V^2)}$	9-8
E	75	$(\pi_1)=\ .4494(\pi_2)^{.7265}(\pi_3)^{.2234}(\pi_4)^{-.4004}(\pi_5)^{1.3555}(\pi_6)^{.1254}(\pi_7)^{-(.0493+.0726\Delta V-.001\Delta V^2)}$	9-9

[a] Value used to derive the equation and $\Delta V=0$ at V^*. (Equations for $V^*=100$ knots are the same as in Table 8.)

Table 10 Summary of percentage errors

Surface type	Velocity knots	Predicted (π_1) using			Actual (π_1)	Percent deviation from actual value		
		Eq. (9-1)	Eq. (9-4)	Eq. (9-7)		Eq. (9-1)	Eq. (9-4)	Eq. (9-7)
A	25	.2496	.2483	.2495	.2496	0	−.5	0
	50	.2008	.1654	.1364	.1654	21.6	0	17.5
	75	.1101	.1088	.1114	.1114	−1.2	−2.3	0
	100	.0736	.0754	.0720	.0720	2.2	4.7	0
		Eq. (9-2)	Eq. (9-5)	Eq. (9-8)		Eq. (9-2)	Eq. (9-5)	Eq. (9-8)
C	25	.5510	.5512	.5509	.5511	0	0	0
	50	.4518	.3644	.2831	.3644	24.0	0	−22.3
	75	.2379	.2374	.2377	.2377	0	0	0
	100	.0971	.0970	.0970	.0970	0	0	0
		Eq. (9-3)	Eq. (9-6)	Eq. (9-9)		Eq. (9-3)	Eq. (9-6)	Eq. (9-9)
E	25	.9730	.9340	.9755	.9730	0	−4.0	.3
	50	.9258	.5856	.3743	.5856	58.0	0	−36.0
	75	.3707	.3571	.3708	.3708	0	−3.7	0
	100	.1053	.1054	.1056	.1054	0	0	0

Table 11 Test conditions

Tire size	d_{tx}	d_{tr}	h in.	A.R.	Infl. PR. psi	Velocity ~ knots	No. of runs
20 in.	A	New	0.02	0.65	300	125 100 75 50 25	5
OD		80%					
(Tire I)		60%					
		40%					
		20%					
		60%	0.04				
			0.06				
			0.08				
			0.10				
			0.06	0.75			
				0.80			
				0.85			
				0.95			
				0.80	250		
					200		
					150		
					100		

85 conditions to be repeated for tires II, III, IV each {30, 40, 50 in. OD}; 85 × 4 conditions to be repeated for surfaces B, C, D, E each; total no. of conditions to be run = 85 × 4 × 5 = 1700; total no. of runs needed if 3 surfaces in one run = 680.

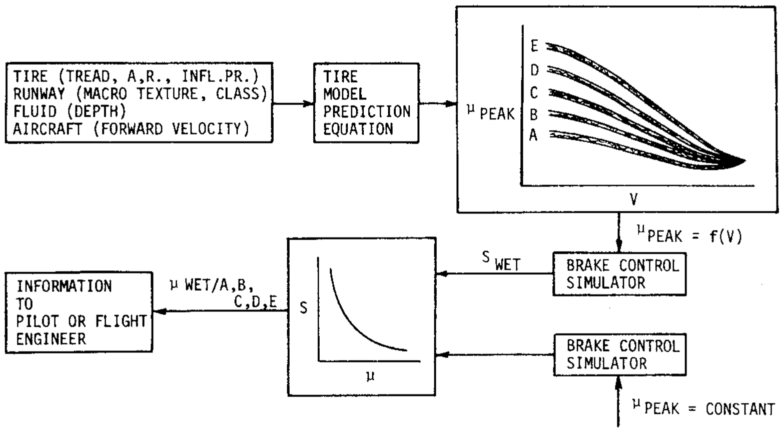

Fig. 7 Use of tire model.

or

$$(\pi_1) = C_\alpha (\pi_2)^\beta (\pi_3)^\gamma (\pi_4)^\delta (\pi_5)^\epsilon (\pi_6)^\zeta (\pi_7)^\eta$$

where exponents β, γ, δ, ϵ, ζ, η, and constant C_α are to be determined from experimental data and additionally C_α is a function of π_2, π_3, π_4, π_5, π_6, and π_7. Thus, information about variables held constant (while varying one at a time) is mandatory to be able to calculate C_α. Engineering judgment (reasonable assumptions) had, therefore, to be made in the present analysis about missing numerical information. Therefore, tests of validity cannot be performed unless test data are collected under fully controlled conditions for all parameters on a given tire. Table 11 shows the number of conditions needed to be run for each tire specimen and each type of surface for a meaningful validation of the tire model.

Having established the prediction equation and assuming its validity, it can then be used along with the brake control simulator (1, 2) for airplane sensitivity study to arrive at the effective μ-wet for a given set of conditions as shown in Fig. 7. This information could then be transmitted to the pilot or the flight engineer or used in a fashion as deemed necessary. The model should be equally applicable to automotive tire-road interface phenomena as the parameters affecting the friction level are very similar.

Conclusions and Recommendations

1) The principal of dimensional analysis can be used to define the runway-tire interface problem and to predict available friction.

2) The prediction equation approach seems to be workable within reasonable tolerances, but more conclusive statements can only be made when more data become available and model validity is tested.

3) Tire test data must be collected under fully controlled conditions. Therefore, a recommended test program must be carried out.

4) In order for the tire model concept to be operationally meaningful, the following areas of work have to be resolved in addition to carrying out the tire test work: classification of runways; runway monitoring system standardization; ground vehicle development and test (Ref. 3); enacting and enforcing regulations regarding proper maintenance of runway friction levels; and method of measuring/indicating rainfall intensity/water depth.

Acknowledgments

This work was conducted under contract F33657-74-C-0129 entitled "Combat Traction II, Phase II, (Extended)." The author thanks the Air Force for funding the project and the Boeing Commercial Airplane Company for permission to publish the paper.

References

[1] Wahi, M. K., Warren, S. M., Amberg, R. L., Attri, N. S., and Straub, H. H., "Combat Traction II, Phase II," Tech. Rept. ASD-TR-74-41, Vol. I and II, Oct. 1974.

[2] Wahi, M. K., "Application of Dimensional Analysis to Predict Airplane Stopping Distance," *Journal of Aircraft*, Vol. 14, Feb. 1977, pp. 209-214.

[3] Wahi, M. K., "A Note on Runway Traction Measurement," *Journal of Tire Science and Technology*, Vol. 5, Aug. 1977, pp. 155-166.

[4] Wahi, M. K. and Straub, H. H., "Tire Runway Interface Friction Prediction Subsystem," Tech. Rept. ASD-TR-77-7, March 1977.

[5] "Aircraft Tire Manual," B. F. Goodrich Aerospace & Defense Products, 1972.

[6] "Aircraft Tire Manual," Goodyear Tire and Rubber Company, 1972.

[7] "Hytrol Skid Control Systems Brochure," Hydro-Aire Division, Crane, Burbank, Calif., 1975.

[8] "Goodyear Brake Control Systems Brochure."

[9] "Jane's All The World's Aircraft," 1973-74.

[10] "1974 Tire & Rim Association Inc. Book," Sec. 9, Akron, Ohio.

[11] Yager, T. J., "A Comparison of Aircraft and Ground Vehicle Stopping Performance on Dry, Wet, Flooded, Slush-Snow and Ice Covered Runways," Final Report on Project-Combat Traction, a Joint USAF-NASA Program. NASA Tech. Note D-6098, Nov. 1970.

[12] "Profiles of Scheduled Air Carrier Airport Operations," "Top 100 U. S. Airports" DOT (FAA) Pub. August 1973.

[13] "Aeronautical Information Publication (AIP) DOT (FAA) Air Traffic Service Flight Services Division," "Aerodromes," AGA No. 2, 5th ed., April 1974.

[14] "Airman's Information Manual," AIP-AGA No. 3, Airport Directory, Part 2, 1974-75.

[15] "DOD Flight Information Publication, IFR-Supplements," United States, Alaska, Pacific & South Asia, Europe, North Africa, and Middle East, 1975.

[16] "DOD Flight Information Publications (Terminal), Instrument Approach Procedures," United States, Alaska, Pacific & South Asia, Europe, North Africa, and Middle East, 1975.

[17] Greech, D. E. and Donald, H. G., "Aircraft Ground Flotation Analysis Procedures—Paved Airfields," Tech. Rept. ASD-TR-70-43, Jan. 1971.

[18] Holmes, T., Lees, G., and Williams, A. R., "A Combined Approach to the Optimization of Tire and Pavement Interaction," *Proceedings of the American Chemical Society*, Miami Beach, April 1971.

[19] Moore, D. F., "The Friction and Lubrication of Elastomers," Pergamon Press, New York, 1972.

[20] "Frictional and Retarding Forces on Aircraft Tires, Part 1: Introduction," Engineering Sciences Data Unit Item 71025, London, Oct. 1971; with Amendment A, Aug. 1972.

[21] Clark, S. L. (Ed.), "Mechanics of Pneumatic Tires," National Bureau of Standards Monograph 122, 1971.

[22] Allbert, B. J and Walker, J. C., "Tire to Wet Road Friction at High Speeds," *Proceedings of Institution of Mechanical Engineers*, Vol. 180, Part 2A, No. 4, 1965-66, pp. 105-158.

[23] Holmes, T. and Gough, V. E., "Wear and Friction of Aircraft Tires," *Proceedings of the Conference on Friction and Wear in Tires*, ERDE, Waltham Abbey, Oct. 1968. Paper 4. Ministry of Technology D. Mat. Rept. 157, June 1969.

[24]Rose, J. G., Hutchinson, J. W., and Gallaway, B. M., "Summary and Analysis of the Attributes of Methods of Surface Texture Measurement," Skid Resistance of Highway Pavements, ASTM STP 530, American Society for Testing and Materials, 1973, pp. 60-77.

[25]"Frictional and Retarding Forces on Aircraft Tires, Part 2: Estimation of Braking Force," ESDU Item No. 71026, London, Oct. 1971, with Amendment A, Aug. 1972.

[26]Horne, W. B., "Results from Studies of Highway Grooving and Texturing at NASA Wallops Station," *Pavement Grooving and Traction Studies,* proceedings of a conference held at Langley Research Center, Hampton, Va., Paper 26, NASA SP-5073, Nov. 1968.

[27]Yager, T. J., "Comparative Braking Performance of Various Aircraft on Grooved and Ungrooved Pavements at the Landing Research Runway, NASA Wallops Station," *Pavement Grooving and Traction Studies,* Proceedings of a conference held at Langley Research Center, Hampton, Va., NASA SP-5073 Paper 3, Nov. 1968.

[28]Leland, T. J. W., Yager, T. J., and Joyner, U. T., "Effects of Pavement Texture on Wet-Runway Braking Performance," NASA TN D-4323, Jan. 1968.

[29]Horne, W. B., Yager, T. J., and Taylor, G. R., "Review of Causes and Alleviation of Low Tire Traction on Wet Runways," NASA TN D-4406, April 1968.

[30]"Tests with a Heavy Load Skidding Test Vehicle Incorporating a Mark Maxaret Anti-Locking Brake System to Determine Braking Force Coefficients Between an Aircraft Tire and Various Wet Surfaces," Trials at the Road Research Track at Crawthrone and at Wisley Aerodrome, White Waltham Aerodrome and London (Heathrow) Airport. Ministry of Aviation S&T Memo, 10/64, Jan. 1965.

[31]Lander, F. T. W. and Williams, T., "The Skidding Resistance of Wet Runway Surfaces with Reference to Surface Texture and Tire Conditions," Road Research Laboratory Rept. 184, 1968.

[32]Yang, N. C., "Design of Functional Pavements," McGraw Hill, New York, 1972.

[33]Murphy, G. C., "Simitude in Engineering," The Ronald Press Co., New York, 1950.

[34]Ludema, K. C. and Gujrati, B. D., "An Analysis of the Literature on Tire-Road Skid Resistance," ASTM Special Tech. Pub. 541, 1973.

[35]Leland, T. J. W. and Taylor, G. R., "An Investigation of the Influence of Aircraft Tire-Tread Wear on Wet-Runway Braking," NASA TN D-2770, 1965.

[36]Williams, T., "Skidding Resistance of Runway Surfaces," *Aircraft Engineering*, Sept. 1971, pp. 6-9.

[37]Dreher, R. C. and Tanner, J. A., "Experimental Investigation of the Cornering Characteristics of a C40X14-21 Cantilever Aircraft Tire," NASA TN D-7203, 1973.

[38]Tanner, J. A. and Dreher, R. C., "Cornering Characteristics of a 40X14-16 Type VII Aircraft Tire and a Comparison with Characteristics of a C40X14-21 Cantilever Aircraft Tire," NASA TN D-7351, 1973.

[39]Harned, J. L., Johnson, L. E., and Scharpf, G., "Measurement of Tire Brake Force Characteristics as Related to Wheel Slip (Antilock) Control System Design," SAE Paper 690214, 1969.